

RSC Advances



This is an *Accepted Manuscript*, which has been through the Royal Society of Chemistry peer review process and has been accepted for publication.

Accepted Manuscripts are published online shortly after acceptance, before technical editing, formatting and proof reading. Using this free service, authors can make their results available to the community, in citable form, before we publish the edited article. This *Accepted Manuscript* will be replaced by the edited, formatted and paginated article as soon as this is available.

You can find more information about *Accepted Manuscripts* in the [Information for Authors](#).

Please note that technical editing may introduce minor changes to the text and/or graphics, which may alter content. The journal's standard [Terms & Conditions](#) and the [Ethical guidelines](#) still apply. In no event shall the Royal Society of Chemistry be held responsible for any errors or omissions in this *Accepted Manuscript* or any consequences arising from the use of any information it contains.

23 **Abstract:**

24 In this article, nanoparticles (NPs) from a water-soluble chitosan (CS) derivative
25 (N-(2-hydroxyl) propyl-3-trimethyl ammonium chitosan chloride, HTCC) and zein
26 had successfully been assembled via a low-energy phase separation method. The
27 fabricated NPs were investigated for the first time to encapsulate and protect
28 curcumin (Cur). The particle size and zeta potential of zein-HTCC NPs varied from
29 66 to 170 nm and +36.3 to +62.5mV, respectively. The encapsulation efficiency (EE)
30 was greatly improved to 94.9% after HTCC coating, compared with 85.2% that using
31 zein as a single encapsulant. The microstructure of the NPs was revealed by
32 transmission electron microscopy (TEM). The physicochemical and structural
33 analysis showed that the electrostatic interactions and hydrogen bonds were major
34 forces responsible for NPs formation. The encapsulation forms were evaluated for
35 their efficiency in overcoming Cur's heat and UV sensitivity, which improve the
36 stability about 2.7 fold, 3.5 fold and 2.5 fold when disposed with 60 °C treatment for
37 30 min, 80 °C treatment for 1 min and ultraviolet radiation for 2 h at zein:
38 HTCC₁=1:1. The results of stability and DPPH assays indicated the protection of
39 bioactivity as encapsulated. Zein-HTCC NPs were believed to be a promising delivery
40 system for supplementation or treatment of hydrophobic nutrients or drugs.

41

42 **Keywords:** zein HTCC curcumin stability protection

43

44

45 **1. Introduction**

46 Bioactive compounds have been intensively investigated in recent years for these
47 health-beneficial properties and for potential applications in the fields of pharmaceutic,
48 nutraceuticals, and functional foods^{1, 2}. Among them, polyphenols have attracted
49 many researchers' attention because of their anti-oxidant, anti-inflammatory, and
50 anti-cancer properties³. Together with some other plant-derived polyphenols, Cur is
51 among the best characterised polyphenols since it is primarily used as a food
52 colourant and more important, it has antioxidant, antibacterial, antifungal, antiviral,
53 anti-inflammatory, antiproliferative, and pro-apoptotic effects⁴⁻⁶. Unfortunately, the
54 application of Cur has been limited by its poor water solubility and instability what is
55 limiting its bioavailability, thus impeding its conversion from cooking to clinical
56 applications^{7, 8}. Therefore, exploitation of Cur as a functional food and nutraceutical
57 ingredient or pharmaceutical compound is feasible only when encapsulated in a
58 delivery system, which is capable of stabilizing and protecting it from degradation
59 while preserving its biological activities and enhancing its bioavailability⁹.

60 Many encapsulation approaches have been applied to increase the water solubility
61 and/or bioavailability of Cur such as liposome¹⁰, polymeric micelles⁷, emulsion¹¹,
62 complex¹², NPs¹³, etc. Among these approaches, biodegradable polymer NPs offer
63 promising enhanced functional properties of bioactive compounds which are unstable
64 against processing and severe storage condition, such as heating, ultraviolet
65 radiation¹⁴. Over the past decades, NPs systems based on proteins including gelatin,
66 collagen, casein, albumin and whey protein have been studied for delivering drugs,

67 nutrients, bioactive peptides and probiotic organisms¹⁵. In most cases, due to the
68 isoelectric point (pI) of protein, the formulations of NPs greatly influenced by the pH
69 condition, making the formulations unstable. Therefore, considerable endeavors have
70 been taken in investigating the associative interactions between natural proteins and
71 polysaccharides in order to improve the stability of NPs¹⁶. As an alcohol-soluble
72 protein obtained from corn, zein has attracted widespread interest in delivery systems
73 due to its inherent excellent biocompatibility and biodegradability¹⁷. Zein has been
74 extensively investigated in the encapsulation of bioactive compounds because of its
75 capability to form self-assembled NPs^{18, 19}. It has thus been utilized in food and
76 pharmaceutical applications, such as heparin, gitoxin, fish oil, and the like²⁰⁻²². CS, a
77 natural polyaminosaccharide obtained from N-deacetylation of chitin, with distinctive
78 biological properties such as non-toxicity, biocompatibility, biodegradability and
79 antimicrobial activity, has been widely used in biomaterial applications¹⁴. However, in
80 neutral and basic environments, the CS molecules lose their charge and precipitation
81 will occur due to the pKa of CS (6.5)²³. To overcome this drawback and expand its
82 use, functional groups have been introduced into CS to make it water-soluble²⁴⁻²⁷.
83 Among the derivatives of CS, quaternized CS has attracted much attention due to the
84 properties of retaining cationic charges at neutral pH, good water solubility,
85 antibacterial activity, mucoadhesivity, enhanced antioxidant activity, and enhanced
86 cellular penetration²⁸. N-(2-hydroxyl) propyl-3-trimethyl ammonium chitosan
87 chloride (HTCC) can be prepared by a relatively easy chemical reaction of CS and
88 2,3-Epoxypropyltrimethyl ammonium chloride (EPTMAC)²⁹. The presence of

89 positive charge is expected to increase the mucoadhesive nature of CS, which leads to
90 an increased residence time and enhanced bioavailability³⁰.

91 In the present work, HTCC with different molecule, which showed higher aqueous
92 solubility than CS in a much broader pH range, was synthesized and used to prepare
93 zein-HTCC NPs. The Cur/zein-HTCC NPs delivery system was developed using a
94 liquid-liquid phase separation approach. The characteristics of Cur encapsulation and
95 protection system have been studied using transmission electron microscopy (TEM),
96 Fourier transform infrared spectroscopy (FT-IR), X-ray diffraction (XRD),
97 fluorescence spectra and DPPH measurements. Additionally, the Cur encapsulation
98 and protection for zein-HTCC NPs were evaluated. Furthermore, the light stability
99 studies of free Cur and Cur/zein-HTCC₁ NPs using the UV absorbance were
100 investigated. The results illustrated zein-HTCC NPs greatly increased the water
101 solubility of Cur and had great potential application for bioactive compounds in food
102 and medicinal fields.

103 **2. Materials and methods**

104 **2.1. Materials**

105 Zein (Mw=19k and 22k Da) was purchased from Tokyo Chemical Industry, Co., Ltd.
106 (Tokyo, Japan). CS with different molecular weight and all with 91% deacetylation
107 were supplied by Zhejiang Yuhuan Ocean Biochemistry Co., Ltd. (China). Curcumin
108 (95.0% purity) was purchased from National Medicine Group Chemical Reagent Co.,
109 Ltd. 2,3-Epoxypropyltrimethyl ammonium chloride (EPTMAC) was purchased
110 from Shandong Dongying Chemical Co., Ltd. with a purity of 96%. Other chemicals

111 used were of analytical grade. All the solutions used in the experiments were prepared
112 using ultrapure water through a Millipore (Millipore, Milford, MA, USA) Milli-Q
113 water purification system.

114 **2.2. Fourier Transform Infrared Spectroscopy (FT-IR) and ¹H-nuclear Magnetic** 115 **Resonance (¹H NMR) spectroscopy**

116 FT-IR spectra were obtained with a Jasco 4100 series with an attenuated total
117 reflection cell (Jasco Inc., Easton, MO). All samples were prepared as KBr pellets and
118 were scanned against a blank KBr pellet background.

119 ¹H NMR spectra were obtained on a Mercury 400 spectrometer (400 MHz for ¹H) in
120 D₂O containing a small amount of CD₃COOD at 25 °C.

121 For pH dependence of the samples water solubility, the test samples (0.5g) were
122 dissolved in 1% HAc (50 ml). With stepwise addition of NaOH solution (1 M), the
123 transmittance of the solutions was recorded with a UV-vis spectrophotometer
124 (UV-1100, MAPADA) at 600 nm.

125 **2.3. Synthesis of HTCC**

126 The HTCC was prepared in a similar manner to the method reported by Lim and
127 Hudson³¹. Briefly, CS (2.0 g, 12.3mmol) was dispersed in isopropyl alcohol (20.0mL)
128 and the solution was adjusted to pH 9, stirring the mixture until the CS was evenly
129 dispersed, heating the solution to 80°C. EPTMAC (11.22 g, 73.8mmol) was dissolved
130 in water and added to CS suspension at 1 h intervals. After reaction for 6 h, the
131 reaction mixture was precipitated by acetone, washed repeatedly until the solution
132 become neutral, dissolved in distilled water. The end-product was obtained by freeze

133 drying after 5-day dialysis.

134 **2.4. Degree of quaternization (DQ)**

135 The DQ of the HTCC was measured by titrating the amount of Cl^- ions on the HTCC
136 with aq AgNO_3 solution. DQ is defined as the mol ratio of bonded EPTMAC per mol
137 of glucosamine calculated from the original mass of CS and its degree of
138 deacetylation (DD)^{31, 32}. Thoroughly dried HTCC (0.1000 g) was dissolved in
139 deionized water (100mL) and conductometrically titrated with 0.017 M AgNO_3 aq
140 solution. Solution conductivities were monitored with conductometer 644 Metrohm,
141 Swiss. During the titration, the temperature of the solution was kept constant
142 (20.4-20.5 °C) using a water bath.

143 **2.5. Molecular weight determination**

144 The average molecular weight (Mw) of quaternized CS was determined by using the
145 gel permeation chromatography (GPC) in conjunction with multi-angle static light
146 scattering detector (DAWN HELEOS II, WYATT, USA) and refractive index detector
147 (Optilab T-rEX, WYATT, USA). All samples were dissolved in acetate buffer (pH 4.5)
148 and then filtered through nylon syringes filters (450nm) (Vertical chromatography Co.,
149 Ltd. Thailand). The mobile phases, 0.5 M AcOH and 0.5 M AcONa (acetate buffer pH
150 4.5), were used at a flow rate of 0.6mL/min at 30°C. Then the injection volume of
151 20 μ L was used.

152 **2.6. Preparation of zein-HTCC NPs and Cur loading**

153 Zein was dissolved in aqueous ethanol solutions (75% v/v) to obtain a stock solution
154 with final concentration of 5mg/mL. HTCC solution was prepared by dissolving

155 weighed HTCC powder into water. Then, 1mL of zein solution was rapidly mixed
156 with 7mL of HTCC solution with different concentration. The solution was under
157 vigorous stirring until a single phase was formed, consisted of different weight ratios
158 of zein: HTCC at 3:1, 2:1, 1:1, 1:2 and 1:3, respectively.

159 For Cur loading, the stock of 20 mg/mL Cur prepared with ethanol was firstly mixed
160 with zein solution for 60 min. The formulation containing Cur was prepared by
161 adding the above solution dropwise to HTCC₁ solution with magnetic stirring,
162 resulting in different weight ratios of zein: HTCC₁ at 3:1, 2:1, 1:1, 1:2 and 1:3,
163 respectively. The finally obtained Cur concentration was 50µg/mL.

164 **2.7. Characterizations of NPs**

165 2.7.1. Particle size and zeta potential

166 Dynamic laser scattering (DLS) and zeta potential measurements of all blank and
167 Cur/zein-HTCC NPs were performed on a commercial laser light scattering
168 instrument (Malvern ZEN3690, Malvern Instruments) at 25°C and 90° scattering
169 angle.

170 2.7.2 Morphology observation

171 Transmission electron microscope (TEM) images were taken on a JEM-2100F (JEOL,
172 Japan). The samples were prepared by dropping solution onto copper grids coated
173 with carbon and then dried naturally.

174 2.7.3. X-ray diffraction (XRD) and fluorescence spectrum

175 Molecular arrangement of Cur, zein and HTCC₁ in powder, as well as the NPs and
176 Cur/zein-HTCC₁ NPs was compared by powder X-ray diffraction patterns acquired at

177 room temperature on a Bruker D8-Advance Diffractometer (Bruker AXS Inc.,
178 Madison, WI, USA) with backgroundless sample holders. The data were collected
179 over an angular range from 5° to 50° 2θ in continuous mode using a step size of 0.02°
180 2θ and step time of 5 seconds.

181 The fluorescence emission spectra of Cur were determined using a Cary Eclipse
182 fluorescence spectrophotometer (Varian Instruments, Walnut Creek, CA) as the
183 excitation wavelength. Cur ($10\mu\text{g/mL}$) was dissolved in ethanol and 10%v/v ethanol.
184 The excitation wavelength was set at 420 nm, and the emission spectra were ranged
185 from 450 to 700 nm. The slit openings were set at 5 nm for both excitation and
186 emission.

187 **2.8. Encapsulation of Cur**

188 Cur in the percolated solutions was determined by a UV-vis spectrophotometer
189 (UV-1100, MAPADA) at 428 nm. The free Cur was obtained by calculating the Cur
190 content that were ultracentrifuged at $4000 \times g$ for 30 min in a refrigerated centrifuge
191 (TGL-20000cR) with angle rotor. The encapsulation efficiency (EE) and loading
192 capacity (LC) were defined as the drug content that was entrapped into zein-HTCC
193 NPs and calculated as follows:

$$194 \quad EE(\%) = \frac{\text{Total Cur} - \text{Free Cur}}{\text{Total Cur}} \times 100$$

$$195 \quad LC(\%) = \frac{\text{Total Cur} - \text{Free Cur}}{\text{Weight of zein - HTCC NPs}} \times 100$$

196 **2.9. Cur protection**

197 To elucidate the effect of encapsulation on the stability of Cur against external severe
198 processing, we compared with remnant content of free Cur with that of entrapped Cur

199 in zein-HTCC NPs after thermal treatment and ultraviolet radiation. Free and
200 encapsulated Cur with concentration of 10 μ g/mL shared pasteurization treatment
201 (60 $^{\circ}$ C, 30 min or 80 $^{\circ}$ C, 1 min) and ultraviolet radiation (30 W, 254 nm) with 40 cm
202 distance was taken into account for the protective effect. For the Cur encapsulated
203 NPs, ethyl alcohol was added and extracted with the same volume for 4 h, and then
204 evaporated overnight at 40 $^{\circ}$ C under vacuum³³. The existent Cur was calculated
205 through the absorption value at 428 nm.
206 For light stability studies, the UV absorbance of free Cur (10 μ g/mL in 10% v/v
207 ethanol) and Cur/zein-HTCC₁ were recorded at 428 nm for 24 h under ambient
208 conditions.

209 **2.10. Radical-scavenging activity by DPPH method**

210 To guarantee the bioactivity of encapsulated Cur, the antioxidant activity of Cur was
211 measured according to the DPPH method with minor modification^{34,35}. Briefly, the
212 scavenging activity assay was carried out by monitoring the absorbance of an
213 ethanolic solution of DPPH (100 μ M) at 517 nm in the presence and absence of the
214 test compounds at room temperature with a UV-vis spectrophotometer. The
215 antioxidant activity of Cur was expressed as the percentage of DPPH that was
216 decreased in comparison with that of the control condition (i.e., the testing solution
217 without the presence of Cur) after 30 min preservation in the dark.

218 **3. Results and discussion**

219 **3.1. Synthesis and characterization of HTCC**

220 In basic aqueous solution, CS with different molecular weight (Mw) was coupled with

221 EPTMAC to give the water-soluble HTCC, in which the amino group of CS was
222 sufficiently nucleophilic to induce ring-opening of EPTMAC (Scheme 1)²³. The Mw
223 and DQ of HTCC were shown in Table 1. The DQ of the HTCC was measured by
224 conductometric titration of Cl^{-1} with 0.017 M aq AgNO_3 solution. The amount of
225 AgNO_3 used at the end point equaled the amount of Cl^{-1} ions presented on the
226 HTCC³¹.

227 The FT-IR spectra of CS and HTCC were measured with KBr pellets in the range of
228 500-3750 cm^{-1} . In the spectrum of HTCC, the characteristic peak (1568 cm^{-1})
229 representing NH_2 deformation was weakened and two new peaks positioned at 1483
230 and 2916 cm^{-1} were appeared (Fig. 1a), which were attributed to the bending mode
231 and flex mode of $-\text{CH}_3$ in quaternized ammonium, indicating that the introduction of
232 the quaternary ammonium salt group on CS backbone^{24, 36}. To further confirm the
233 success of the reaction, ^1H NMR analysis of CS and HTCC was performed in
234 $\text{CD}_3\text{COOD}-\text{D}_2\text{O}$. The NMR spectra of the samples were shown in Fig. 1b and Fig. 1c.
235 As evidence of the reaction, methyl groups in the quaternary ammonium salt group
236 were observed as a very strong peak at 3.2 ppm.

237 Fig. 1d showed the pH dependence of CS and HTCC solutions. At low pH (pH < 6.0),
238 the transmittance was close to 100% not only for the HTCC solution but also for the
239 CS solutions. When the pH increased from 6.0 to 7.0, the transmittance of the CS
240 solution rapidly dropped, and the solution became opaque. In contrast, the
241 transmittance of HTCC solution did not changed. These results illustrated that HTCC
242 has a better solubility in neutral and basic conditions than CS³².

243 3.2. Optimization of the Formulation

244 Due to cationic properties of HTCC, zein can be investigated to form NPs with HTCC
245 to develop novel drug delivery systems. The effects of preparation parameters on
246 particle size and zeta potential in different formulations were summarized in Table 2
247 and Table 3.

248 The particle size of Cur-encapsulated zein NPs without HTCC₁ coating was 134 nm.
249 After HTCC₁ coating was applied on zein NPs, the particle size varied with the weight
250 ratios of zein and HTCC₁. With the increase of HTCC₁ ratios, particle size of
251 Cur/zein-HTCC₁ NPs increased from around 66 to 156 nm. At zein-HTCC₁ ratio of
252 3:1, 2:1 and 1:1, the particle size was even lower than of the zein NPs which might be
253 due to the reason that opposite surface charge of zein and HTCC₁ could let these two
254 kinds of compounds more close to each other³⁷. Besides, the NPs had a small PDI less
255 than 0.16 except for Cur/zein NPs which had a greater PDI of 0.25. The zeta potential
256 of Cur/zein NPs was -17.3 mV. After coated by HTCC₁, the zeta potential of NPs
257 became highly positive in the range of +36.3 to +42.8 mV which slightly augmented
258 with the increase of HTCC₁ concentrations. These observations confirmed that
259 HTCC₁ was successfully coated on the surface of Cur/zein NPs by electrostatic
260 interactions. The encapsulation efficiency (EE) of different formulations was also
261 demonstrated in Table 2. The EE of zein NPs without HTCC₁ was around 85.2% and
262 increased to 92.7% at a zein-HTCC₁ ratio of 1:1 (Table 2). This could be ascribed to
263 the HTCC₁ through electrostatic interactions, resulting in the thick and dense
264 Cur/zein- HTCC₁ NPs and therefore an increase of EE.

265 The effect of HTCC Mw on the NPs size, zeta potential, PDI, EE and LC was also
266 investigated (Table 3). The size increased as Mw of HTCC increased (the ratio of zein:
267 HTCC was kept at 1:1). This phenomenon might be due to longer molecular chains of
268 HTCC with larger Mw entangled with negatively charged zein NPs through ionic
269 interactions would give rise to bigger complex. Moreover, zeta potential increased
270 with the HTCC Mw. This observation can be easily explained by the stronger
271 electrostatic interaction between HTCC and zein. Higher Mw of HTCC with higher
272 degree of quaternization was expected to provide more positive charge and compact
273 NPs because a greater number of trimethylammonium groups of HTCC interacted
274 with zein NPs. Moreover, the wide distribution led to an increase in PDI. Seen from
275 Table 3, higher Mw of HTCC led to higher EE because the longer chain of HTCC
276 molecule could entrap more Cur²⁷.

277 **3.3. Influence of pH on zein NPs and zein-HTCC₁ NPs**

278 To study the effect of pH on the precipitation kinetics of zein NPs and zein-HTCC₁
279 NPs, all samples were studied by dispersing the pre-formed formations in deionized
280 water adjusted to pH from 2 to 11 using 0.1 N HCl or 0.1 N NaOH. Zein has an
281 isoelectric pH of 6.2 and hence the particles have tendency to aggregate at
282 neutral-basic pH. At pH 6 of the zein NPs solution, the precipitation appeared (Fig.
283 2a). However, it kept small particle size and PDI for zein-HTCC₁ NPs at this pH (Fig.
284 2b). The zeta potential of zein NPs was positive at pH <6, while the zeta potential was
285 negative at pH >7 (Fig. 2a). At acid condition, the decrease in the zeta potential of
286 zein-HTCC₁ might be due to the stronger ion strength, leading to the charge screening

287 effect. Moreover, at highly alkaline pH value, the decline of the zeta potential of
288 zein-HTCC₁ NPs was attributed to the augment of zeta potential (negative charge) of
289 zein NPs. The similar observation was also revealed in other studies^{37,38}. The particle
290 size of zein-HTCC₁ NPs kept almost constant from pH 3 to 10 (Fig. 2b). The PDI in
291 the whole pH range (2-11), was less than 0.2. Our finding was that the zein-HTCC₁
292 NPs were stable at a broad range of pH, which was an appealing advantage for further
293 application.

294 **3.4. Morphological Observation**

295 The morphological observation of zein NPs, zein-HTCC₁ NPs and Cur/zein-HTCC
296 NPs were performed by TEM. Figure 3a showed a typical size distribution profile of
297 zein NPs. TEM micrograph displayed that zein NPs without HTCC coating shared
298 features of a spherical shape (Fig. 3b). After zein NPs were coated by HTCC₁, the
299 complex formed sphere NPs with smooth surface and much smaller and more
300 homogeneous diameter (Fig. 3c and 3d). The reduced particle size might be
301 contributed by the electrostatic interactions between zein NPs and HTCC₁ molecules.
302 As shown in Fig. 3e-3i, the incorporation of Cur did not cause morphological changes.
303 With the Mw of HTCC increased, the size of NPs increased. The TEM diameter of the
304 NPs was smaller than that obtained from DLS. This phenomenon may be due to the
305 inherent difference in detection of the particle size between DLS and TEM. DLS
306 provides the data of the NPs swollen in solution, whereas that obtained by TEM
307 showed the images of the NPs spread and dried on copper grids coated with carbon
308 film^{39, 40}.

309 3.5. FT-IR, XRD and fluorescence spectrum

310 Figure 4a showed spectra of zein, zein-HTCC₁ NPs, Cur/zein NPs and Cur/zein-
311 HTCC₁ NPs. In the original spectra of zein (Fig. 4a) and HTCC (Fig. 1a), the bands of
312 hydrogen bonds were at 3441, and 3477 cm⁻¹, respectively. However, after formation
313 of NPs, shift of hydrogen bonds occurred, and the peaks were at 3422, 3432, 3438
314 cm⁻¹ in the spectra of zein-HTCC₁ NPs, Cur/zein NPs and Cur/zein-HTCC₁ NPs
315 respectively, suggesting the hydrogen bonding was formed between Cur and zein, zein
316 and HTCC₁. Therefore, the hydrogen bonding among zein, HTCC, and Cur was
317 considered to be one of the major forces facilitating NPs formation. The amide I band
318 of zein at 1646 cm⁻¹ showed the prominent C=O stretching and the amide II band at
319 1549cm⁻¹ involving C-N stretching. It shifted significantly to 1639 and 1541 cm⁻¹,
320 respectively in Cur/zein NPs, suggesting that the electrostatic interactions were
321 another intermolecular force between Cur and zein. Compared with zein, the bands of
322 amide I and amide II groups shifted to 1655 and 1542 cm cm⁻¹, respectively, in
323 zein-HTCC₁ NPs, indicating the electrostatic interactions between zein and HTCC₁. A
324 further shift of these bands occurred after Cur was encapsulated into NPs. Besides,
325 because both zein and Cur are highly hydrophobic molecules, the hydrophobic
326 interactions could also contribute to the formation of NPs.

327 The XRD patterns of the NPs and pure Cur were shown in Figure 4b. The major
328 characteristic peaks of Cur were at appeared at 8.90, 12.26, 14.54, 17.24, 23.33, 24.60
329 and 25.52 degree, indicative of their highly crystalline nature⁴¹. In contrast, zein
330 showed two flatter humps instead of sharp peaks, indicating the amorphous nature of

331 the protein⁴². Cur specific peaks disappeared in all the formations of suggesting that
332 Cur in the NPs or the complex did not exist as a crystal form which provided
333 additional evidence of encapsulation.

334 Considering that Cur itself is a fluorescent compound, and the fact that the
335 fluorescence spectrum of a compound is usually affected by its microenvironment, we
336 compared the emission spectrum of Cur in zein-HTCC NPs with that of Cur in
337 ethanol and 10%v/v ethanol. Cur has very poor water solubility (11ng/mL) and is a
338 major factor that limits its in vivo bioavailability. Zein-HTCC₁ NPs significantly
339 increased the water solubility of Cur, as evidenced from the evident increase in Cur
340 fluorescence compared to the free Cur in 10%v/v ethanol (Figure 4c). The
341 fluorescence of Cur in zein-HTCC₁ NPs was lower than the fluorescence of Cur in
342 100% ethanol which also was another evidence for encapsulation. The emission peak
343 of Cur in ethanol was at 542 nm, while the peak shifted to 531 nm when Cur was
344 encapsulated in zein-HTCC₁ Cur. This result further confirmed that the
345 microenvironment of Cur was changed upon Cur-encapsulation⁴.

346 **3.6. Cur protection**

347 As we know, Cur's applications are limited due to its low water solubility and
348 sensitivity to alkaline conditions, thermal treatment, ultraviolet radiation, metallic ions,
349 enzymes, oxygen and ascorbic acid, thus restricting its bioavailability⁴³. However,
350 pasteurization and radiation sterilization were common technologies in food
351 processing industry. The thermal and ultraviolet and light stability of encapsulated Cur
352 was estimated in comparison to non-encapsulated Cur (Fig. 5a). After 60 °C treatment

353 for 30 min, 80 °C treatment for 1 min and ultraviolet radiation for 2 h, the unchanged
354 Cur was reduced to 21.9%, 29.2% and 24.5%, respectively for free Cur (Fig. 5a).
355 When Cur was loaded into zein NPs, the retention of Cur was 74.5%, 73.5% and
356 60.4%, respectively (Fig. 5a). Interestingly, the zein/HTCC₁ NPs protective effect was
357 more obvious. When the weight ratio of zein/HTCC₁ was 1:1, the Cur preserved could
358 reach to 79.2%, 77.3% and 60.5%, respectively, when subjected 30 min 60 °C
359 treatment, 1 min 80 °C treatment and 2 h ultraviolet radiation (Fig. 5a). Compared
360 with free Cur at the same treatments, the zein/HTCC₁ protected Cur content was
361 enhances about 2.7 fold, 3.5 fold and 2.5 fold. However, in the same proportion,
362 protective effect had no further increased as the Mw increased (Fig. 5a). The results
363 clearly showed that the stability of encapsulated Cur at the weight ratio of zein:
364 HTCC₁ = 1:1, could be protected and improved, which was helpful to broaden Cur
365 potential application in the food field. As can be seen from Figure 5b, the absorbance
366 of free Cur decreased rapidly to 50% within 30 min, while the absorbance of Cur in
367 zein-HTCC₁ NPs decreased gradually and the absorbance was seen up to 12h(Fig. 5c).
368 The light stability of Cur was enhanced dramatically after encapsulation in
369 zein-HTCC₁ NPs.

370 **3.7. Antioxidant activity**

371 Antioxidants can scavenge free radicals and maintain its safety, nutritional quality,
372 functionality and palatability by retarding the process of lipid peroxidation, which is
373 one of the major reasons for deterioration of food and pharmaceutical products during
374 processing and storage⁴⁴. Cur is a natural compound reported to possess strong

375 antioxidant activity. In our study, we used the DPPH scavenging method to verify the
376 radical-scavenging ability of zein-HTCC NPs loaded Cur. Without any treatment in
377 control group, the antioxidative effectiveness of disposed Cur was lower than that of
378 free Cur (Fig. 6), indicating its instability in food process, which has been found in
379 previous studies and consistent with above results⁴⁵. The antioxidant activity of free
380 Cur was about 72.2%, revealing the higher antioxidant activity, while the scavenging
381 rate decreased to 39.9%, 41.6% and 30.6% with 60 °C treatment for 30 min, 80 °C
382 treatment for 1 min and ultraviolet radiation for 2 h (Fig. 6). When encapsulated into
383 zein NPs, under the same treatments, the antioxidant activity increased as compared
384 with the free Cur except for free Cur in control group without any treatment (Fig. 6).
385 Comparatively, the Cur/zein-HTCC NPs was given a higher antioxidant activity in the
386 same conditions. Moreover, in the weight ratio of zein: HTCC₁ = 1:1, the DPPH
387 radical-scavenging ability of protected Cur were improved 13.3%, 26.9% and 29.0%
388 compared with free Cur, when the solutions were pasteurized at low and high
389 temperature and ultraviolet radiation respectively (Fig. 6). However, with the Mw
390 increased, the antioxidant activity did not further enhanced, which also co-responded
391 with the protection experiments (Fig. 6). The obtained results confirmed that the
392 loaded Cur still retained its free radical scavenging ability, even after it had been
393 subjected to an encapsulation.

394 **4. Conclusion**

395 In this work, zein-HTCC NPs was fabricated successfully as a novel delivery system
396 for Cur, using a low-energy liquid-liquid dispersion method. By coating Cur/zein NPs

397 with HTCC, particle size was dramatically changed and zeta potential was increased
398 to be highly positive, depending on Mw of HTCC. Hydrogen bonding and
399 electrostatic interaction as well as hydrophobic interaction were considered to be the
400 major forces facilitating the formation of NPs. Cur was encapsulated in zein-HTCC
401 NPs, improving its solubility and stability and preserving its bioactivity in
402 pasteurization and ultraviolet radiation, which broadened its application in functional
403 foods and medical field. The worthwhile endeavor elucidated
404 proteins/polysaccharides complex was feasible to solubilize and protect sensitive
405 amphiphilic bioactive compounds and has extensive potential in food and medicinal
406 application with various purposes.

407

408 **Acknowledgements**

409 This work was financially supported by the National Natural Science Foundation of
410 China (No. 31071607). The authors would like to express their sincere gratitude to
411 many conveniences offered by colleagues of Key Laboratory of Environment
412 Correlative Dietology of Huazhong Agricultural University.

413

414

415

416

417

418

419 **References**

- 420 1. L. Liang and M. Subirade, *The Journal of Physical Chemistry B*, 2010, **114**,
421 6707-6712.
- 422 2. G. Jayaprakasha, L. Jaganmohan Rao and K. Sakariah, *Food Chem.*, 2006, **98**,
423 720-724.
- 424 3. R. Pegg and F. Shahidi, *Food Science and Technology-New York-Marcel*
425 *Dekker*, 2004, **167**, 509.
- 426 4. H. Yu and Q. Huang, *Food Chem.*, 2010, **119**, 669-674.
- 427 5. K. Parvathy, P. Negi and P. Srinivas, *Food Chem.*, 2009, **115**, 265-271.
- 428 6. W. Wu, J. Shen, P. Banerjee and S. Zhou, *Biomaterials*, 2011, **32**, 598-609.
- 429 7. M. Esmaili, S. M. Ghaffari, Z. Moosavi-Movahedi, M. S. Atri, A. Sharifzadeh,
430 M. Farhadi, R. Yousefi, J. M. Chobert, T. Haertlé and A. A.
431 Moosavi-Movahedi, *LWT-food science and technology*, 2011, **44**, 2166-2172.
- 432 8. S. Shishodia, M. M. Chaturvedi and B. B. Aggarwal, *Curr. Probl. Cancer*,
433 2007, **31**, 243-305.
- 434 9. M. Sessa, R. Tsao, R. Liu, G. Ferrari and F. Donsi, *J. Agric. Food. Chem.*, 2011,
435 **59**, 12352-12360.
- 436 10. S. S. Dhule, P. Penfornis, T. Frazier, R. Walker, J. Feldman, G. Tan, J. He, A.
437 Alb, V. John and R. Pochampally, *Nanomed. Nanotechnol. Biol. Med.*, 2012, **8**,
438 440-451.
- 439 11. K. Ahmed, Y. Li, D. J. McClements and H. Xiao, *Food Chem.*, 2012, **132**,
440 799-807.

- 441 12. W. Xu, W. Jin, C. Zhang, Z. Li, L. Lin, Q. Huang, S. Ye and B. Li, *Food Res.*
442 *Int.*, 2014, **59**, 61-66.
- 443 13. M. M. Yallapu, B. K. Gupta, M. Jaggi and S. C. Chauhan, *J. Colloid Interface*
444 *Sci.*, 2010, **351**, 19-29.
- 445 14. A. R. Dudhani and S. L. Kosaraju, *Carbohydr. Polym.*, 2010, **81**, 243-251.
- 446 15. A. Sadeghi, F. Dorkoosh, M. Avadi, P. Saadat, M. Rafiee-Tehrani and H.
447 Junginger, *Int. J. Pharm.*, 2008, **355**, 299-306.
- 448 16. T. Moschakis, B. S. Murray and C. G. Biliaderis, *Food Hydrocolloids*, 2010,
449 **24**, 8-17.
- 450 17. A. R. Patel and K. P. Velikov, *Current Opinion in Colloid & Interface Science*,
451 2014, **19**, 450-458.
- 452 18. S. Lee, N. S. A. Alwahab and Z. M. Moazzam, *Int. J. Pharm.*, 2013, **454**,
453 388-393.
- 454 19. Y. Luo and Q. Wang, *J. Appl. Polym. Sci.*, 2014, **131**, 40696.
- 455 20. H. J. Wang, Z. X. Lin, X. M. Liu, S. Y. Sheng and J. Y. Wang, *J. Controlled*
456 *Release*, 2005, **105**, 120-131.
- 457 21. L. Muthuselvi and A. Dhathathreyan, *Colloids Surf. B. Biointerfaces*, 2006, **51**,
458 39-43.
- 459 22. Q. Zhong, H. Tian and S. Zivanovic, *J. Food Process. Preserv.*, 2009, **33**,
460 255-270.
- 461 23. A. Wan, Q. Xu, Y. Sun and H. Li, *J. Agric. Food. Chem.*, 2013, **61**, 6921-6928.
- 462 24. S. H. Zhao, X. T. Wu, W. C. Guo, Y. M. Du, L. Yu and J. Tang, *Int. J. Pharm.*,

- 463 2010, **393**, 269-273.
- 464 25. Y. Chang, L. Xiao and Y. Du, *Polym. Bull.*, 2009, **63**, 531-545.
- 465 26. C. Liu, Y. Tan, C. Liu, X. Chen and L. Yu, *J. Ocean Univ. China*, 2007, **6**,
- 466 237-243.
- 467 27. S. Shu, L. Sun, X. Zhang, Z. Wu, Z. Wang and C. Li, *J. Nanopart. Res.*, 2011,
- 468 **13**, 3657-3670.
- 469 28. Y. Cheng, H. Cai, B. Yin and P. Yao, *Int. J. Pharm.*, 2013, **454**, 425-434.
- 470 29. V. Mourya and N. N. Inamdar, *J. Mater. Sci. Mater. Med.*, 2009, **20**,
- 471 1057-1079.
- 472 30. T. Sonia and C. P. Sharma, *Carbohydr. Polym.*, 2011, **84**, 103-109.
- 473 31. S. H. Lim and S. M. Hudson, *Carbohydr. Res.*, 2004, **339**, 313-319.
- 474 32. Z.-X. Peng, L. Wang, L. Du, S. R. Guo, X. Q. Wang and T. T. Tang, *Carbohydr.*
- 475 *Polym.*, 2010, **81**, 275-283.
- 476 33. A. Kumar and M. Ahuja, *Carbohydr. Polym.*, 2012, **90**, 637-643.
- 477 34. Y. J. Shang, X. L. Jin, X. L. Shang, J. J. Tang, G. Y. Liu, F. Dai, Y. P. Qian, G. J.
- 478 Fan, Q. Liu and B. Zhou, *Food Chem.*, 2010, **119**, 1435-1442.
- 479 35. O. Suwantong, P. Opanasopit, U. Ruktanonchai and P. Supaphol, *Polymer*,
- 480 2007, **48**, 7546-7557.
- 481 36. W. Li, L. Xiao and C. Qin, *Journal of materials science*, 2010, **45**, 5915-5922.
- 482 37. Y. Luo, B. Zhang, M. Whent, L. L. Yu and Q. Wang, *Colloids Surf. B.*
- 483 *Biointerfaces*, 2011, **85**, 145-152.
- 484 38. S. Podaralla and O. Perumal, *AAPS PharmSciTech*, 2012, **13**, 919-927.

- 485 39. G. Wang, B. Yu, Y. Wu, B. Huang, Y. Yuan and C. S. Liu, *Int. J. Pharm.*, 2013,
486 **446**, 24-33.
- 487 40. K. Zhu, T. Ye, J. Liu, Z. Peng, S. Xu, J. Lei, H. Deng and B. Li, *Int. J. Pharm.*,
488 2013, **441**, 721-727.
- 489 41. A. Patel, Y. Hu, J. K. Tiwari and K. P. Velikov, *Soft Matter*, 2010, **6**, 6192.
- 490 42. Y. Luo, T. T. Wang, Z. Teng, P. Chen, J. Sun and Q. Wang, *Food Chem.*, 2013,
491 **139**, 224-230.
- 492 43. B. H. Lee, H. A. Choi, M.-R. Kim and J. Hong, *Food Science and*
493 *Biotechnology*, 2013, **22**, 279-282.
- 494 44. T. Ak and İ. Gülçin, *Chem. Biol. Interact.*, 2008, **174**, 27-37.
- 495 45. E. I. Paramera, S. J. Konteles and V. T. Karathanos, *Food Chem.*, 2011, **125**,
496 913-922.
- 497
- 498
- 499
- 500
- 501
- 502
- 503
- 504
- 505
- 506

507 **Figure captions:**

508 Fig.1 FT-IR spectra of CS and HTCC (a). ^1H NMR spectra data of CS (b) and HTCC (c). pH
509 dependence of water solubility of CS and HTCC (d); the concentrations of CS and HTCC are 1%
510 (w/v). CS represented the one made for HTCC. HTCC represented the Mw of 8.708×10^3 . Data
511 were displayed as mean \pm SD (n=3).

512

513 Fig.2 Effect of pH on particle size, zeta potential and PDI from 2 to 11.0 on zein NPs and zein-
514 HTCC₁ NPs prepared at zein: HTCC₁ ratio of 1: 1 w/w. Digital photographs were shown inset.
515 Data were displayed as mean \pm SD (n=3).

516

517 Fig.3 Size distribution of zein NPs (a) and zein-HTCC₁ NPs (c) prepared at zein: HTCC₁ ratio of
518 1:1 w/w. TEM photos of zein NPs (b) and zein-HTCC₁ NPs (d). TEM images of zein- HTCC₁ NPs
519 (e), zein-HTCC₂ NPs (f), zein-HTCC₃ NPs (g), zein-HTCC₄ NPs (h), zein-HTCC₅ NPs (i) at
520 zein-HTCC ratio of 1:1 w/w with the concentration of Cur at 50 $\mu\text{g}/\text{mL}$.

521

522 Fig.4 FT-IR (a) and XRD (b) of different samples. Cur, curcumin powder; zein, zein powder;
523 zein-HTCC₁, zein-HTCC₁ NPs prepared using zein: HTCC₁ ratio of 1: 1 w/w; Cur/zein,
524 curcumin-loaded zein NPs at curcumin concentration of 50 $\mu\text{g}/\text{mL}$; Cur/zein-HTCC₁,
525 curcumin-loaded zein-HTCC₁ NPs prepared using zein: HTCC₁ ratio of 1: 1 w/w at curcumin
526 concentration of 50 $\mu\text{g}/\text{mL}$. Fluorescence spectra of curcumin (10 $\mu\text{g}/\text{mL}$) in ethanol, 10% ethanol
527 solution and Cur-loaded zein-HTCC₁ NPs solution (Cur equivalent of 10 $\mu\text{g}/\text{mL}$) (c).

528

529 Fig.5 Cur protection by zein-HTCC with different Mw of HTCC at the zein-HTCC ratio of 1:1
530 w/w in the heat and ultraviolet treatment (a). Absorbance of Cur (10 μ g/mL) in 10% ethanol
531 solution (b) and Cur-loaded zein-HTCC₁ NPs (Cur equivalent of 10 μ g/mL) solution (c) as a
532 function of time. Data were displayed as mean \pm SD (n=3).

533

534 Fig.6 Radical scavenging activity improvement by Cur entrapment with different Mw of HTCC at
535 the zein-HTCC ratio of 1:1 w/w. Control group indicated samples without any treatments. Data
536 were displayed as mean \pm SD (n=3).

537

538

539

540

541

542

543

544

545

546

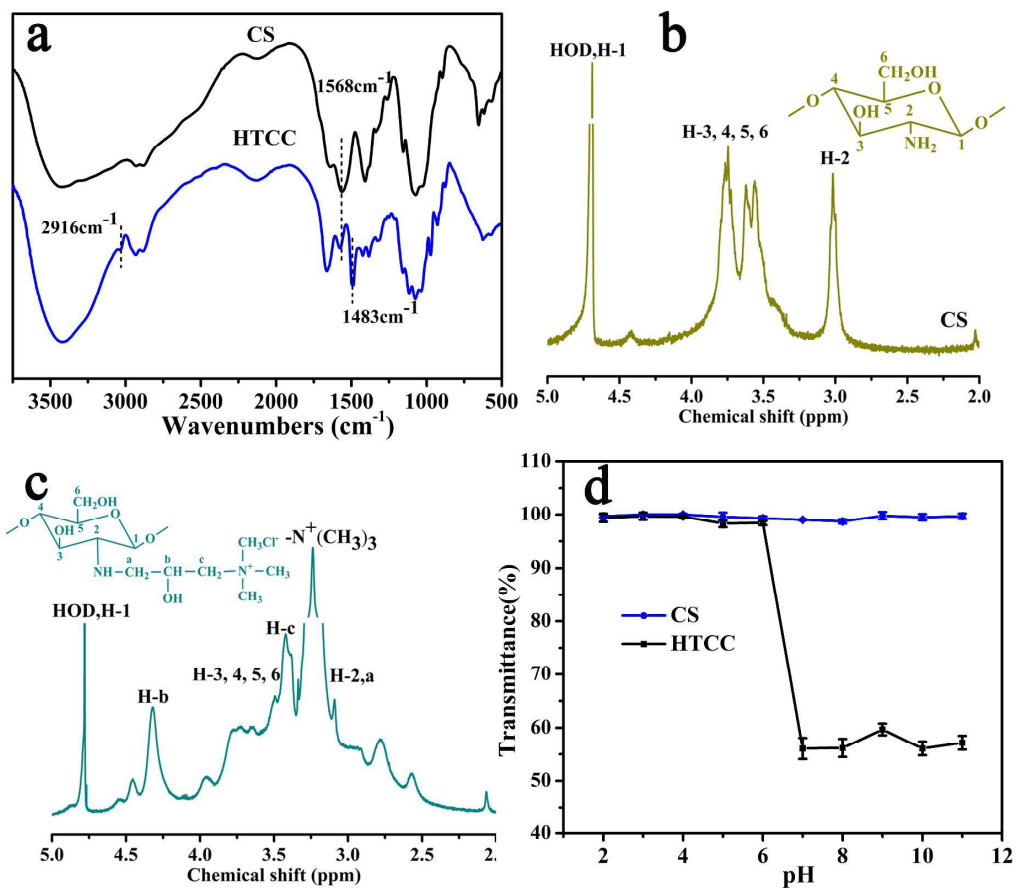
547

548

549

550

551 Fig.1



552

553

554

555

556

557

558

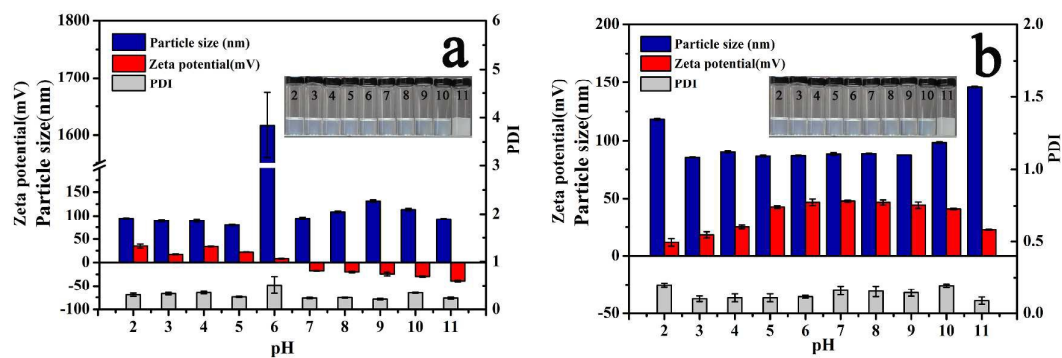
559

560

561

562

563 Fig.2



564

565

566

567

568

569

570

571

572

573

574

575

576

577

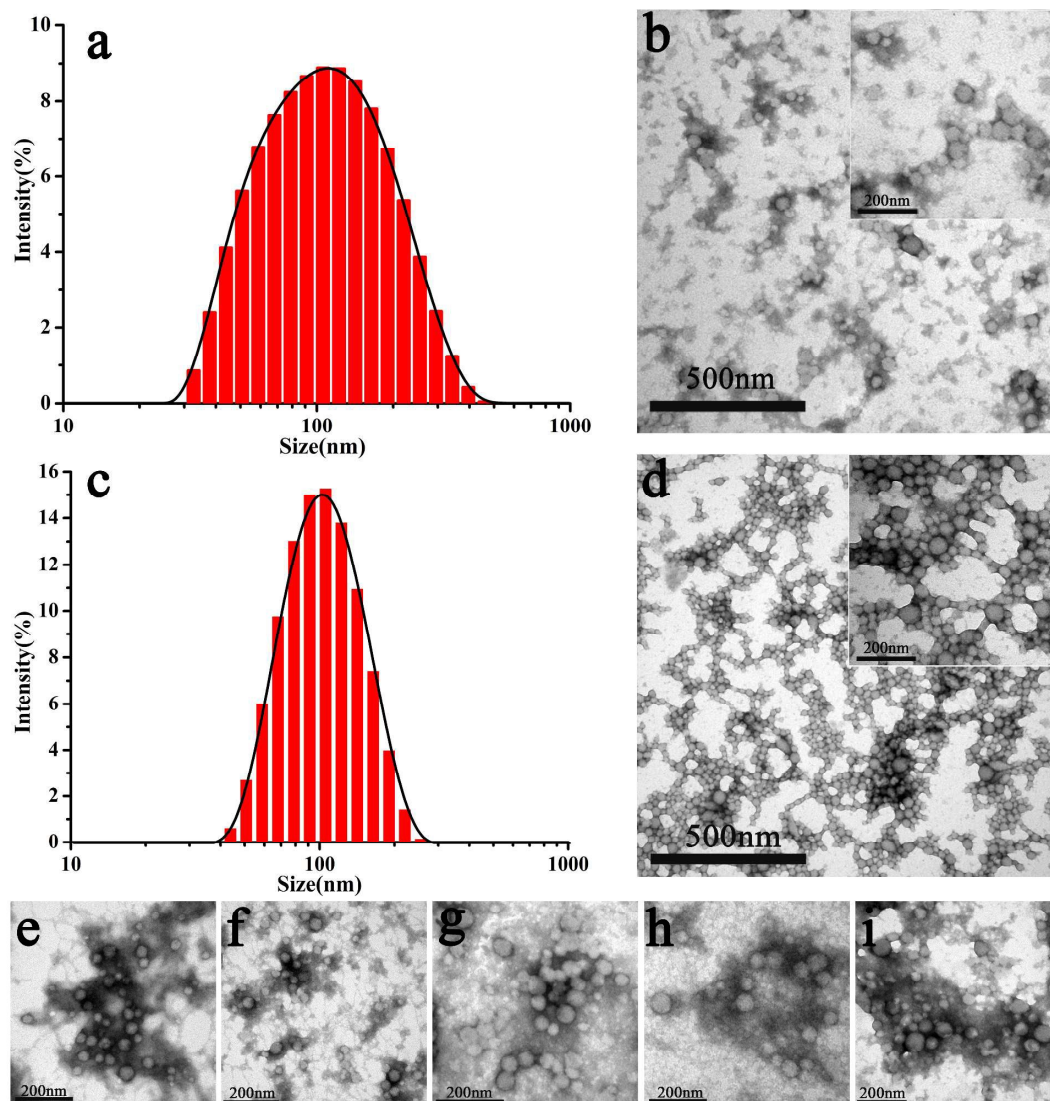
578

579

580

581

582 Fig.3



583

584

585

586

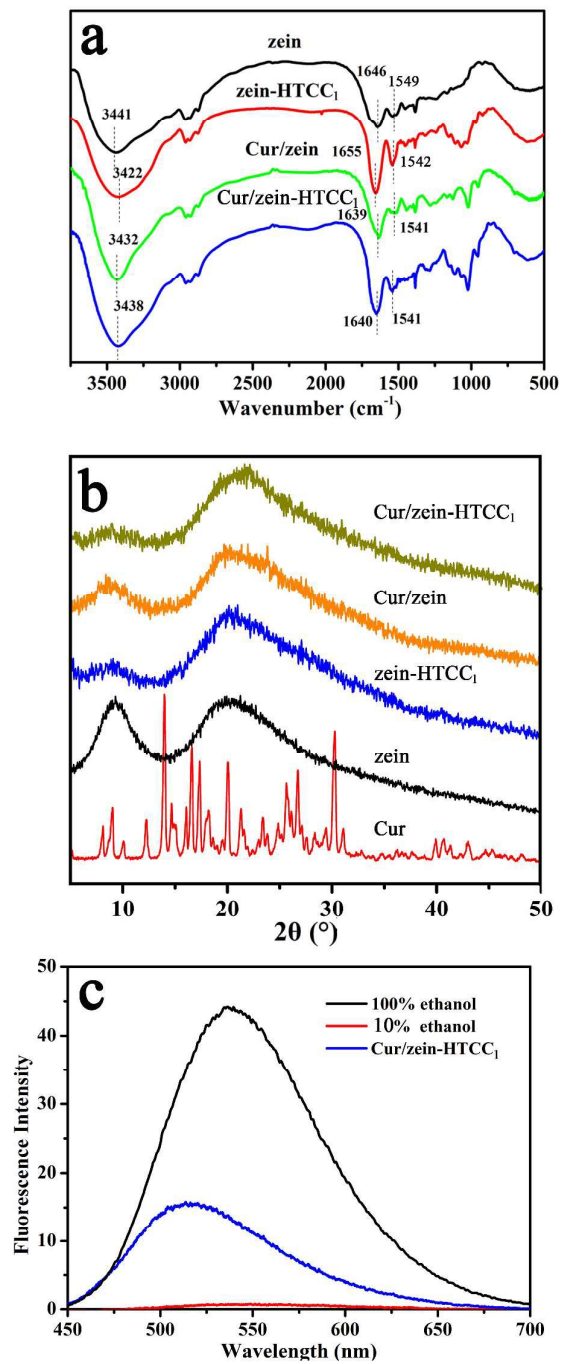
587

588

589

590

591 Fig.4



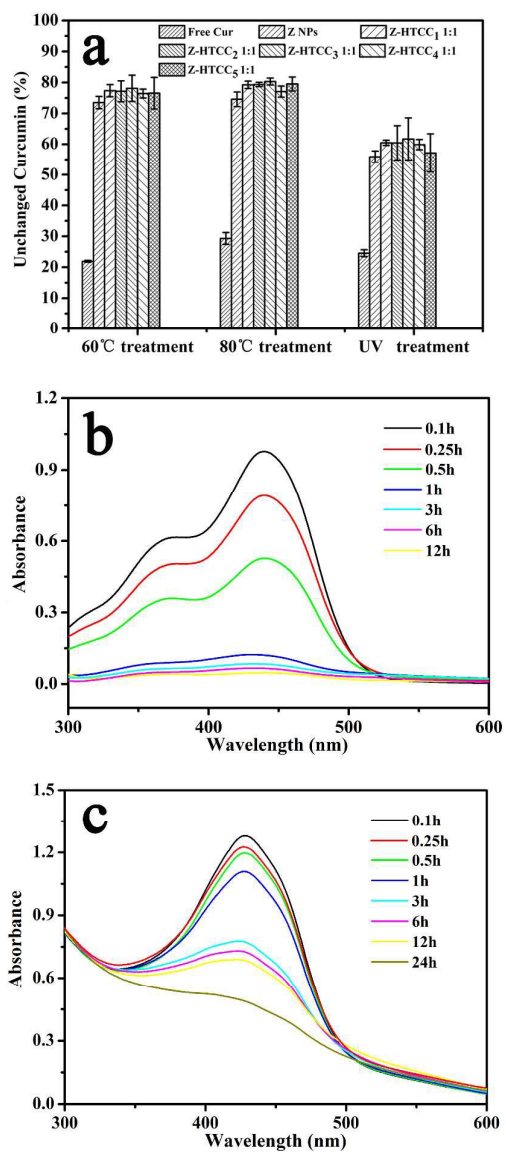
592

593

594

595

596 Fig.5



597

598

599

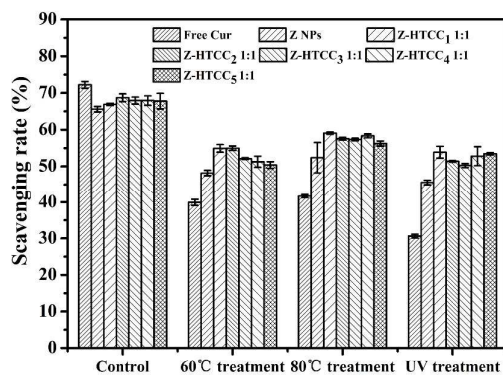
600

601

602

603

604 Fig.6



605

606

607

608

609

610

611

612

613

614

615

616

617

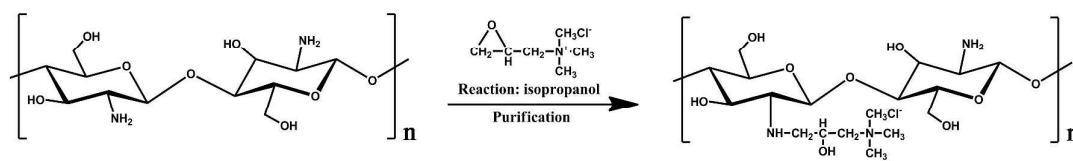
618

619

620

621

622 Scheme 1



Scheme 1. Synthesis of the HTCC

643 Table 1

644

Table 1 Properties of HTCC

Sample	Degree of quaternization	M_w
HTCC ₁	0.623±0.02	8.708×10^3
HTCC ₂	0.869±0.03	1.688×10^5
HTCC ₃	0.879±0.04	3.322×10^5
HTCC ₄	0.907±0.03	7.051×10^5
HTCC ₅	0.921±0.05	1.832×10^6

645 HTCC₁-HTCC₅ represented HTCC with different quaternization degree and different molecular

646 weight. Data were displayed as mean±SD (n=3).

647

648

649

650

651

652

653

654

655

656

657

658

659

660

661

662 Table 2

663 Table 2 Effect of zein: HTCC₁ weight ratios on the size, PDI, zeta potential, EE and

664 LC of NPs

Samples	Size(nm)	PDI	Zeta potential(mV)	EE(%)	LC(%)
Z	134.8±2.9	0.25±0.02	-17.3±1.5	85.2±1.2	8.5±0.12
Z-HTCC ₁ 3:1	66.4±0.30	0.15±0.01	36.3±0.6	87.7±1.2	6.5±0.11
Z-HTCC ₁ 2:1	79.1±0.30	0.14±0.02	37.9±0.6	89.4±2.4	5.7±0.16
Z-HTCC ₁ 1:1	121.0±1.6	0.13±0.01	38.3±3.8	92.7±1.7	4.4±0.08
Z-HTCC ₁ 1:2	154.0±2.0	0.13±0.03	39.0±0.6	89.7±2.4	2.8±0.08
Z-HTCC ₁ 1:3	156.3±1.8	0.16±0.05	42.8±1.3	86.8±4.1	2.0±0.10

665 Z represents zein NPs without HTCC coating with the concentration of Cur at 50µg/mL. Other

666 samples represent formulations with different mass ratios of zein-HTCC₁ with the concentration of

667 Cur at 50µg/mL. PDI, polydispersity. EE (%), encapsulation efficiency. LC (%), loading capacity.

668 Data were displayed as mean±SD (n=3).

669

670

671

672

673

674

675

676

677

678

679

680 Table 3

681 Table 3 Effect of HTCC Mw on the size, PDI, zeta potential, EE and LC of NPs

Samples	Size(nm)	PDI	Zeta potential(mV)	EE(%)	LC(%)
Z-HTCC ₂ 1:1	105.1±2.1	0.29±0.04	48.6±3.1	92.9±3.9	4.4±0.10
Z-HTCC ₃ 1:1	141.9±7.0	0.36±0.06	49.1±2.6	93.5±2.4	4.4±0.06
Z-HTCC ₄ 1:1	158.3±3.1	0.48±0.03	54.2±4.7	93.9±1.2	4.4±0.08
Z-HTCC ₅ 1:1	177.0±4.3	0.52±0.03	62.5±1.2	94.9±1.9	4.5±0.08

682 Samples represent formulations with different Mw of HTCC at the zein-HTCC ratio of 1:1 with

683 the concentration of Cur at 50µg/mL. PDI, polydispersity. EE (%), encapsulation efficiency.

684 LC(%), loading capacity. Data were displayed as mean±SD (n=3).

685

686

687